

Model Based Transition Control for Biplane Tailsitter

Shubhangshu Gupta* and Sreekar Doranala † and Mangal Kothari ‡ and Abhishek §

Indian Institute of Technology Kanpur, Kanpur, India, 208016

Tailsitter aircrafts, a class of hybrid unmanned aerial vehicles (UAVs), experience significant challenges during transition due to its highly nonlinear dynamics. This paper proposes a model based tracking control approach to address this limitation. The rapidly changing attitude and airspeed during transition make conventional controller design methods challenging. This work presents a method to generate optimal transition trajectories using a simplified 3 degree-of-freedom (3-DOF) model of the aircraft. A nonlinear dynamic inversion (NDI) based feedback controller is proposed for trajectory tracking during forward and backward transitions. The proposed NDI is validated through simulations and demonstrates successful trajectory tracking during transitions under wind disturbances and parameter uncertainties. The NDI controller enables efficient transition without altitude loss, facilitating seamless mode changes between hover and fixed-wing flight.

I. Nomenclature

c	= chord
C_L, C_D	= nondimensional lift and drag coefficients
C_{L_0}, C_{D_0}	= lift and drag coefficient at zero angle of attack
C_{L_α}	= lift curve slope
C_m	= nondimensional pitching moment coefficient
C_{m_0}	= pitching moment coefficient at zero angle of attack
C_{m_α}	= moment curve slope
$F_{a_x}, F_{a_y}, F_{a_z}$	= components of wing aerodynamic force in body-fixed axis
g	= acceleration due to gravity
J	= inertia tensor of the vehicle
L, D	= lift and drag forces
l, m, n	= rolling, pitching and yawing moments due to rotors
\bar{m}	= mass of the vehicle
M_a	= wing aerodynamic pitching moment
p, q, r	= vehicle angular velocity components along body-fixed axis
S	= wing area
T	= thrust
v_x, v_y, v_z	= vehicle velocity components along inertial axis
V_c, α_c	= Vehicle velocity and angle of attack during a trim cruise flight
V_∞	= vehicle velocity with respect to surrounding air
x, y, z	= inertial position co-ordinates
ω	= vehicle angular velocity
ϕ, θ, ψ	= Euler angles
α	= wing angle of attack
ρ	= atmospheric air density

*Graduate Student, Dept. of Aerospace Engineering, Indian Institute of Technology Kanpur, Kanpur, India.

†Graduate Student, Dept. of Aerospace Engineering, Indian Institute of Technology Kanpur, Kanpur, India.

‡Professor, Dept. of Aerospace Engineering, Indian Institute of Technology Kanpur, Kanpur, India.

§Professor, Dept. of Aerospace Engineering, Indian Institute of Technology Kanpur, Kanpur, India.

II. Introduction

IN recent years, the sector of unmanned aerial vehicles (UAVs) has witnessed significant advancements. UAVs have the capability to be used in a diverse range of applications, from urban areas for photography and infrastructure inspection, to rural areas for crop monitoring and fertilizers spraying, and even in defense sector for patrolling, search, and rescue operations. The list of applications continues to expand, as does the research on UAV development. However, the UAVs based on conventional aircraft designs have their own limitations [1, 2]. While rotary UAVs have a limited range and endurance, fixed-wing UAVs require considerable space for take off and landing (TOL) operations. This has led researchers to explore hybrid configurations for UAVs, which aim to synergize the advantages of both rotary and fixed-wing designs [2–6]. These hybrid UAVs, also known as transitioning UAVs, have the unique ability to operate in both vertical takeoff and landing (VTOL) and fixed-wing flight modes. Apart from the two conventional flight states, there exist intermediate transition states to toggle between hovering and fixed-wing flight. The overall reliability of a hybrid UAV is directly dependent on its ability to perform a smooth transition, as successful maneuvering during this stage is essential for safe and efficient operation.



Fig. 1 Biplane tailsitter designed at Helicopter lab, Department of Aerospace Engineering, IIT Kanpur

Biplane tailsitter (Fig. 1) is one such class of hybrid UAV which is a prime interest of this work due to its minimal mechanical complexity. This design features a quadrotor system with two wings positioned normal to the plane of the rotors. The transition is achieved with a full rigid-body rotation about its pitch axis. This makes the same rotor system enabled during complete flight regime, thereby eliminating the need for redundant actuation system. However, this mechanically simple system comes at a cost of complex aerodynamic maneuvers during transition. The high angle of attack and low speed maneuvers during this phase make the vehicle susceptible to stall and loss of altitude.

Currently available transition methods, such as those employed by PX4 *, an open source autopilot firmware, rely on open loop control. A constant throttle command is provided, along with a constant pitchrate or a constant pitch setpoint command for forward and backward transition, respectively[7]. While these reference, after tuning, could pilot the vehicle to transit between the flight modes, they often end up with unnecessary throttle usage and altitude gain.

This lack of precision has motivated the researchers to explore trajectory planning and model based control strategies for the transition flight.

Optimal trajectory planning for tailsitter UAV involves generating a feasible flight path that incorporates system dynamics of the vehicle. This process requires a performance index that needs to be optimized, such as minimizing control efforts [8], reducing transition time [9], or maintaining the altitude [10]. Additionally, multiple constraints like terminal velocity and attitude must also be included into the planning process. Tracking this reference trajectory requires a reliable controller design. While conventional controller designs cater to either multicopter or fixed-wing flight, designing a controller for transitioning flight phase in tailsitters is challenging. This difficulty arises as the model cannot be linearized around any single trim point. Furthermore, the rotor thrust and aerodynamic forces exhibit highly nonlinear behavior due to high angle of attack encountered during transitions, leading to nonlinear flight dynamics. The Authors in [11] proposed a method that utilises pre-computed reference thrust and pitch trajectories, feeding it directly to the attitude controller, eliminating the need of outer loop position controller. Similarly, a feedforward control trajectory of rotor thrust and pitch attitude is parameterized as a polynomial function by [12], the polynomial coefficients are then optimized through iterative flight tests. A feedback controller was proposed by [13] to address uncertainties arising while using only feedforward commands. The authors in [14] implemented a linear quadratic regulator (LQR) controller on error dynamics of a monowing tailsitter. This approach, however, focussed solely on the velocities in the translational dynamics, neglecting the inertial position effect.

While previous efforts have explored the control laws for transition of tailsitter vehicles, major of the work relied on attitude controller of the UAV for transition, utilizing either a feedforward trajectory, or a linearized error control. To the authors' knowledge, a complete trajectory tracking using a dedicated model based outer loop controller has not been explored. This distinction allows for a more comprehensive and adaptable approach to trajectory tracking during the

*https://docs.px4.io/main/en/flight_stack/controller_diagrams.html#vtol-flight-controller

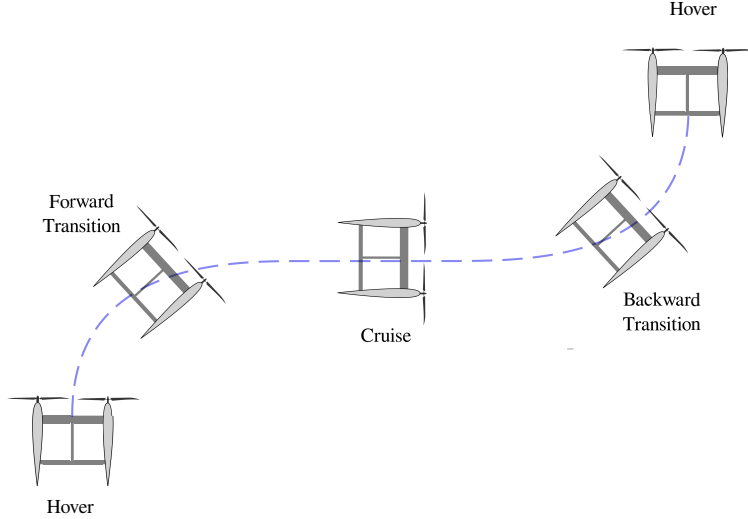


Fig. 2 Forward and backward transitions of quadrotor biplane tailsitter.

transition maneuver. The major contribution of the presented work can be highlighted as follows:

- 1) Forward and backward transition trajectories are generated based on optimal trajectory generation method.
- 2) A nonlinear dynamic inversion based trajectory tracking control is presented, which improves tracking performance, enabling successful transition with desired terminal speed and attitude, without significant loss or gain of altitude.
- 3) Inner loop attitude control based on geometric control is implemented, which is based on attitude dynamics in special orthogonal group, SO(3).
- 4) The proposed controller is tested in presence of wind disturbances, and parameter uncertainties of mathematical model.

The rest of the article is arranged as follows: A brief description of the tailsitter design used for this paper and its dynamic model is presented in Section III. Optimal trajectory generation problem is formulated in Section IV. Section V presents the complete control scheme for the proposed controller. Section VI presents the results and discusses on the trajectory tracking performance. Finally, the paper concludes in Section VII.

III. Vehicle Equation of Motion

A. Vehicle Description

The biplane quadrotor vehicle is essentially a conventional quadrotor configuration with two wings attached perpendicular to the plane of the rotors, as shown in Fig. 1. The vehicle takes off as a quadrotor, relying solely on the rotors for actuation. After taking off the entire body gradually tilts forward about its pitch axis while accelerating along the body z axis. Once the required speed and pitch attitude are achieved, the vehicle shifts to fixed-wing flight, where the wings provide the lift needed to sustain its weight. The various flight modes for the tailsitter can be seen in Fig. 2.

A mathematical model of biplane quadrotor tailsitter UAV is designed by aligning the quadrotor frame with inertial North-West-Up (NWU) frame for ease of observation. As the wing aerodynamic forces are low due to low translational speeds, only rotors are used as actuators during transition. Therefore, it is convenient to use quadrotor frame for deriving the mathematical model of the UAV. The equations of motion are standard 6-degree-of-freedom (6-DOF) equations. Translational dynamics is modeled in inertial frame, while the rotational dynamics is modeled in body frame and corresponding Euler angle frames. As the conventional 3-2-1 parameterization sequence has a singularity at $\theta = \pm\pi/2$, the rotation matrix is obtained from quadrotor body frame to inertial frame following the 3-1-2 sequence. In this case singularity appears at $\phi = \pm\pi/2$, which is far from the operating point of the vehicle. Using the updated sequence, the relation between the components of a vector in body-fixed frame and inertial frame can be given as

$$v_i = R_b^i v_b, \quad (1)$$

where v_i and v_b represent the coordinate form of vector v in inertial frame and body-fixed frame, respectively, and $R_b^i \in SO(3)$ is a rotation matrix from body-fixed frame to inertial frame. Following the 3-1-2 sequence, R_b^i is obtained

as

$$R_b^i = \begin{bmatrix} \cos \theta \cos \psi - \sin \theta \sin \phi \sin \psi & -\cos \phi \sin \psi & \sin \theta \cos \psi + \cos \theta \sin \phi \sin \psi \\ \cos \theta \sin \psi + \sin \theta \sin \phi \cos \psi & \cos \phi \cos \psi & \sin \theta \sin \psi - \cos \theta \sin \phi \cos \psi \\ -\sin \theta \cos \phi & \sin \phi & \cos \theta \cos \phi \end{bmatrix}. \quad (2)$$

B. Kinematics

The translational velocity of the UAV is expressed in inertial coordinate frame. The kinematic relationship between the displacement and rate vectors (both linear and angular) can be given as

$$\begin{bmatrix} \dot{x} \\ \dot{y} \\ \dot{z} \end{bmatrix} = \begin{bmatrix} v_x \\ v_y \\ v_z \end{bmatrix}, \quad (3)$$

$$\begin{bmatrix} p \\ q \\ r \end{bmatrix} = \begin{bmatrix} \cos \theta & 0 & -\sin \theta \cos \phi \\ 0 & 1 & \sin \phi \\ \sin \theta & 0 & \cos \theta \cos \phi \end{bmatrix} \begin{bmatrix} \dot{\phi} \\ \dot{\theta} \\ \dot{\psi} \end{bmatrix}. \quad (4)$$

C. Dynamics

The net force experienced by the UAV includes gravitational, aerodynamic and propulsive forces. Similarly, the net moment contains aerodynamic and propulsive forces and moments. The translational dynamics (in inertial frame) and rotational dynamics (in body frame) can be modeled as

$$\begin{bmatrix} \dot{v}_x \\ \dot{v}_y \\ \dot{v}_z \end{bmatrix} = R_b^i \left(\begin{bmatrix} 0 \\ 0 \\ T/\bar{m} \end{bmatrix} + \frac{1}{\bar{m}} \begin{bmatrix} F_{a_x} \\ F_{a_y} \\ F_{a_z} \end{bmatrix} \right) + \begin{bmatrix} 0 \\ 0 \\ -\bar{m}g \end{bmatrix}, \quad (5)$$

$$\begin{bmatrix} \dot{p} \\ \dot{q} \\ \dot{r} \end{bmatrix} = J^{-1} \left(\begin{bmatrix} l \\ m \\ n \end{bmatrix} + \begin{bmatrix} 0 \\ M_a \\ 0 \end{bmatrix} - \begin{bmatrix} p \\ q \\ r \end{bmatrix} \times J \begin{bmatrix} p \\ q \\ r \end{bmatrix} \right). \quad (6)$$

Aerodynamic forces are calculated first in wind frame, and then transformed to body frame.

$$\begin{bmatrix} F_{a_x} \\ F_{a_y} \\ F_{a_z} \end{bmatrix} = \begin{bmatrix} \cos \alpha & 0 & \sin \alpha \\ 0 & 1 & 0 \\ -\sin \alpha & 0 & \cos \alpha \end{bmatrix} \begin{bmatrix} -L \\ 0 \\ -D \end{bmatrix}, \quad (7)$$

where,

$$\begin{aligned} L &= \frac{1}{2} \rho V_\infty^2 S C_L(\alpha), \\ D &= \frac{1}{2} \rho V_\infty^2 S C_D(\alpha), \\ M_a &= \frac{1}{2} \rho V_\infty^2 c S C_m(\alpha). \end{aligned} \quad (8)$$

As the transition is performed in longitudinal plane and at a low velocity, the lateral aerodynamic forces and moments have been ignored in the work.

IV. Trajectory Generation

The goal of trajectory generation is to obtain a feasible and optimal flight path which depends on the dynamics of the vehicle in use, while also taking physical constraints into account. This helps in optimizing power consumption and maximizing efficiency, in addition to ensuring a smooth transition between hover and cruise flight. This is crucial to avoid sudden changes in attitude, speed or altitude that could destabilize the vehicle.

As the UAV performs transition in its body x-z plane, a simplified 3-D dynamic model has been used for the transition trajectory generation. The vehicle state includes the position and velocity in inertial frame, and pitch and pitchrate in corresponding frames ($X = [x \ z \ v_x \ v_z \ \theta \ \dot{\theta}]^\top$). The control inputs are the wing rotor thrust ($U = [U_1 \ U_2]^\top$). The subsequent procedure is based on the lines of the method from [8].

A. Optimization Problem

A general optimal control problem poses the problem of finding state and control trajectory such that a performance index \mathcal{J} is optimized, subject to system dynamics and design constraints.

$$\begin{aligned} \underset{X, U}{\operatorname{argmin}} \quad & \mathcal{J} = F(X, U, t), \\ \text{s.t. } & \dot{X} = f(X, U), \\ & X(T_0) = X_0, \\ & g(X, U) \leq 0. \end{aligned} \quad (9)$$

For the transition problem, following optimal control problem is formulated

$$\mathcal{J} = \Phi(X_f, T_f) + \int_{T_0}^{T_f} \mathcal{L}(X, U) dt. \quad (10)$$

The running cost \mathcal{L} and terminal cost Φ are given by

$$\begin{aligned} \mathcal{L}(X, U) &= \left(U_1 - \frac{1}{2} \bar{m}g \cos(\theta) \right)^2 + \left(U_2 - \frac{1}{2} \bar{m}g \cos(\theta) \right)^2, \\ \Phi(X_f) &= (X_f - X_d)^\top Q_f (X_f - X_d), \end{aligned} \quad (11)$$

where $X_f = X(T_f)$ represents the state at the end of transition and X_d denotes the desired terminal state. The matrix $Q_f \in \mathbb{R}^{6 \times 6}$ is a positive semidefinite diagonal matrix, which serves as the weight matrix used to penalize the deviation of the state from the desired terminal state.

B. Trajectory Plots

The optimal control problem, as described in Eq. (9) and equipped with appropriate constraints, serves the purpose of deriving forward and backward transition trajectories for the UAV. The optimization problem is formulated and solved using nonlinear programming (NLP) method using the software package CasADi [15]. The terminal condition and weight gains selected are detailed in Table 1. Here, cruise velocity and angle-of-attack during cruise flight are determined to be $V_c = 14m/s$ and $\alpha_c = 3^\circ$. These values are attained by solving trim conditions for a fixed-wing flight.

Table 1 Parameter selection for forward and backward transition

Parameters	Forward transition	Backward transition
X_d	$[\text{free}, V_c, 0, 0, (\pi/2 - \alpha_c), 0]^\top$	$[\text{free}, 0, 2, 0, 0, 0]^\top$
Q_f	$\text{diag}([0, 120, 20, 100, 100, 100])$	$\text{diag}([0, 120, 20, 100, 100, 100])$
T_f	3.5 s	3.5 s

The optimal transition trajectories for forward and backward transition are shown in Fig. 3 and Fig. 4, respectively. Figure 3a illustrates the forward transition in inertial frame, where the arrows depicts the attitude of the vehicle. The optimal control inputs are displayed in Fig. 3b, and remaining states are shown in Fig. 3c and 6c. Similarly, the plots for the backward transition are presented in Fig. 4.

V. Control Architecture

Generally, forward and backward transition for a tailsitter UAV are performed using an open loop controller, i.e., the position controller is disabled during the transition process. A reference thrust and pitch setpoint trajectory is provided,

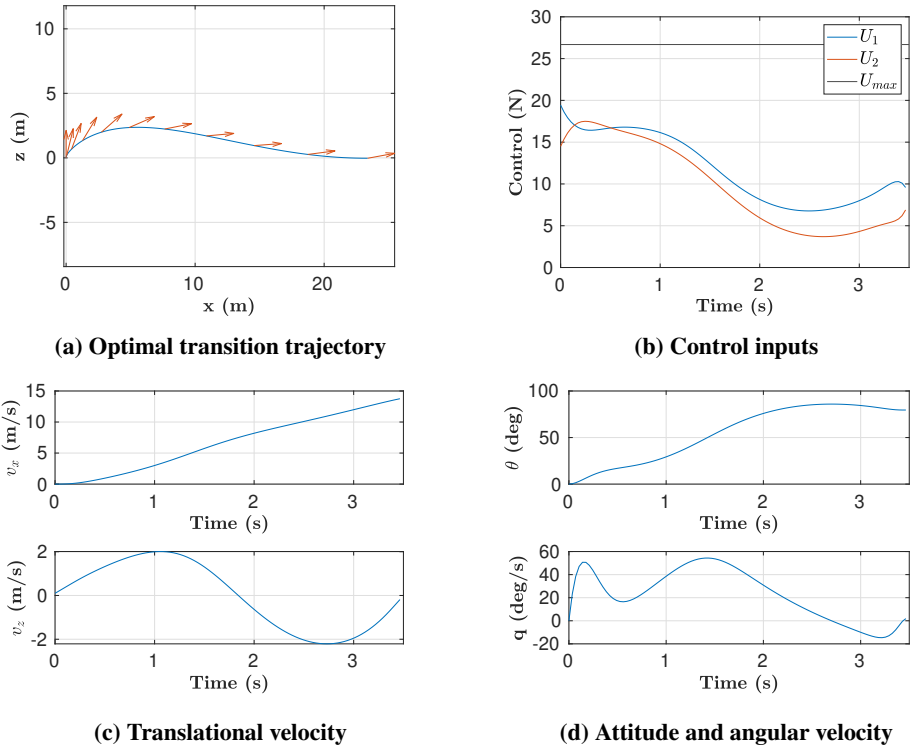


Fig. 3 Optimal transition trajectory for forward transition

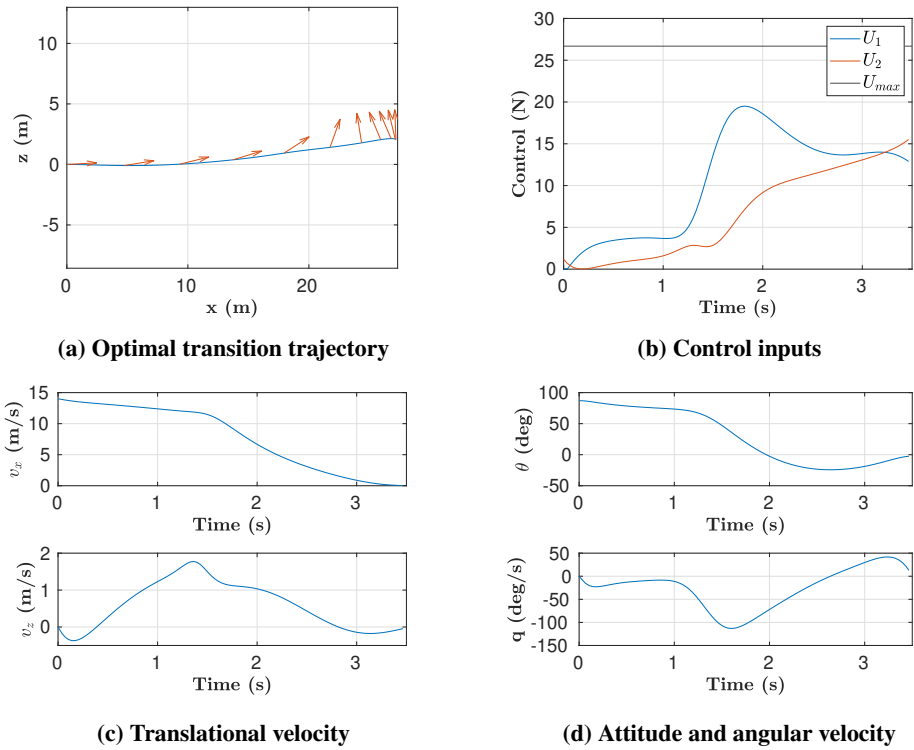


Fig. 4 Optimal transition trajectory for backward transition

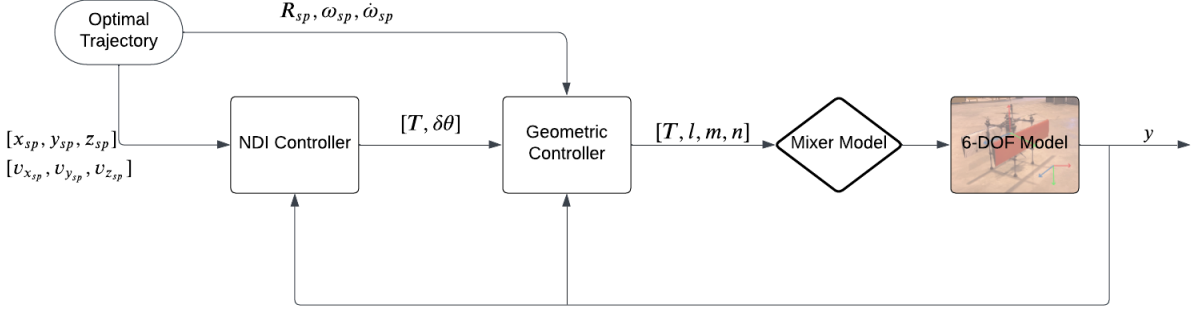


Fig. 5 Control scheme for transition

and low level attitude control attempts to follow the setpoint. The setpoint trajectory is either a simplified constant throttle and pitchrate command [16], or it is derived from solving optimization problems [7].

In the current work, the reference trajectory is tracked using outer loop velocity control based on nonlinear dynamic inversion (NDI). The outerloop provides thrust and attitude setpoints. These setpoints are utilised by the inner loop attitude control, which operates on geometric control architecture. The complete control structure is presented in Fig. 5.

A. Nonlinear Dynamic Inversion based Controller

A generic NDI based controller acting as outer loop is proposed as in [17], that provides the desired thrust as output. It also provides correction in attitude trajectory from the reference pitch setpoints available. The NDI controller depends on the translational dynamics of the system to follow the generated reference trajectory. The nonlinear translational dynamics of the UAV, as shown in Eqs. (3) and (5), can be written as

$$\begin{aligned} \dot{X}_1 &= X_2, \\ \dot{X}_2 &= \frac{1}{\bar{m}} (R_b^i F_a - W + U), \end{aligned} \quad (12)$$

where $X_1 = [x, y, z]$ and $X_2 = [v_x, v_y, v_z]$ are inertial position and velocity of the UAV, respectively, F_a represents the aerodynamic force in body-fixed frame, W represents the gravitational force in inertial frame, and U represents the control input in inertial frame. Equation 12 represents the system dynamics in companion form.

1. Error Dynamics

For trajectory tracking problem, let X_d , \dot{X}_d and \ddot{X}_d define the optimal translational trajectory, where X_d is the desired inertial position of UAV. Defining the error state as

$$\begin{aligned} e_1 &= X_1 - X_d, \\ e_2 &= X_2 - \dot{X}_d, \end{aligned} \quad (13)$$

transforms the system dynamics into state error dynamics as

$$\begin{aligned} \dot{e}_1 &= e_2, \\ \dot{e}_2 &= \frac{1}{\bar{m}} (R_b^i F_a - W + U) - \ddot{X}_d \end{aligned} \quad (14)$$

We define a virtual control input \mathbf{v} as

$$\mathbf{v} \triangleq \frac{1}{\bar{m}} (R_b^i F_a - W + U) - \ddot{X}_d \iff U = \bar{m}(\mathbf{v} + \ddot{X}_d) + W - R_b^i F_a. \quad (15)$$

The virtual control input cancels the nonlinearity in the system and convert the system into a linear model of form $\dot{x} = Ax + Bv$. We aim to find virtual control \mathbf{v} which could converge the tracking error to zero.

$$\begin{bmatrix} \dot{e}_1 \\ \dot{e}_2 \end{bmatrix} = \begin{bmatrix} 0_{3 \times 3} & I_{3 \times 3} \\ 0_{3 \times 3} & 0_{3 \times 3} \end{bmatrix} \begin{bmatrix} e_1 \\ e_2 \end{bmatrix} + \begin{bmatrix} 0 \\ I_{3 \times 3} \end{bmatrix} v. \quad (16)$$

2. Control Objective

A full state feedback controller can be implemented on the given linearised system.

Lemma 1. For any initial error $e_1 = e(0)$ and state feedback control input $v = -[K_1, K_2][e_1, e_2]^\top$, the error dynamics governed by the Eq. (16) asymptotically converges to zero.

Proof. Substituting the state feedback control in the error dynamics Eq. 16, we obtain

$$\begin{bmatrix} \dot{e}_1 \\ \dot{e}_2 \end{bmatrix} = \begin{bmatrix} 0_{3 \times 3} & I_{3 \times 3} \\ 0_{3 \times 3} & 0_{3 \times 3} \end{bmatrix} \begin{bmatrix} e_1 \\ e_2 \end{bmatrix} + \begin{bmatrix} 0 \\ I_{3 \times 3} \end{bmatrix} \left(-[K_1, K_2] \begin{bmatrix} e_1 \\ e_2 \end{bmatrix} \right), \quad (17)$$

$$\begin{bmatrix} \dot{e}_1 \\ \dot{e}_2 \end{bmatrix} = \begin{bmatrix} 0_{3 \times 3} & I_{3 \times 3} \\ -K_1 & -K_2 \end{bmatrix} \begin{bmatrix} e_1 \\ e_2 \end{bmatrix} \quad (18)$$

The eigen values of the closed loop error dynamics can be obtained as

$$\begin{aligned} \begin{vmatrix} \lambda I_{3 \times 3} & -I_{3 \times 3} \\ K_1 & \lambda I_{3 \times 3} - K_2 \end{vmatrix} &= 0, \\ \det(\lambda I_3 + (K_2 + \lambda I_3)^{-1} K_1) \det(K_2 + \lambda I_3) &= 0. \end{aligned} \quad (19)$$

The eigen values are obtained as

$$\lambda^2 + K_{2i}\lambda + K_{1i} = 0 \quad \forall i \in \{1, 2, 3\}. \quad (20)$$

Since K_{1i} and K_{2i} are positive, the matrix in Eq. (18) is Hurwitz, and hence it can be concluded that the dynamics governed by Eq. 16 is asymptotically stable. \square

Once the virtual control input v is obtained, the actual control input U can be obtained by substituting in Eq. 15.

$$U = \bar{m}(-K_1 e_1 - K_2 e_2) + \bar{m} \ddot{X}_d + W - R_b^i F_a. \quad (21)$$

The control input obtained is in inertial frame, which can be transformed into body-fixed frame using the transformation matrix.

$$\begin{bmatrix} F_{b_x} \\ F_{b_y} \\ F_{b_z} \end{bmatrix} = R^\top U. \quad (22)$$

Since the thrust actuation is available only in body z-axis, a correction in attitude is required to align the body z-axis with the direction in which net thrust is required. Performing the vector rotation of body thrust into desired direction, we obtain

$$\begin{aligned} T &= \sqrt{F_{b_x}^2 + F_{b_y}^2 + F_{b_z}^2}, \\ \delta\phi_d &= \sin^{-1} \left(\frac{F_{b_y}}{T} \right), \\ \delta\theta_d &= \sin^{-1} \left(\frac{F_{b_x}}{T \cos(\delta\phi_d)} \right) \approx \sin^{-1} \left(\frac{F_{b_x}}{T} \right). \end{aligned} \quad (23)$$

The UAV is expected to move in $y = 0$ plane. Hence, desired roll and yaw attitude are obtained to be zero in reference trajectory ($\phi_d = \psi_d = 0$). Any deviation from the planar trajectory is called as cross track error. The final attitude setpoints can be obtained as

$$\begin{aligned} \phi_{sp} &= \phi_d + \delta\phi = \delta\phi_d, \\ \theta_{sp} &= \theta_d + \delta\theta_d, \\ \psi_{sp} &= \tan^{-1} \left(\frac{v_y}{v_x} \right). \end{aligned} \quad (24)$$

B. Geometric Controller

The geometric attitude controller works on SO(3) manifold, and hence, the desired attitude from optimal trajectory is given as a rotation matrix $R_d(\phi_d, \theta_d, \psi_d)$. The corrections in desired attitude generated from outer loop control is used to update the desired attitude. The Euler rates are converted to obtain angular velocity in body-fixed frame. As Euler 3-1-2 rotation sequence is used to for transformation, singularity at $\phi = \pi/2$ does not appear into picture, as can be seen in Eq. (4). The geometric controller architecture is adapted from [12]. The control moments, as a function of attitude error and error in angular velocity, can be given as

$$M = J\dot{\omega} + \omega \times (J\omega) - M_{aero} - K_R e_R - K_\Omega \Omega_e, \quad (25)$$

where J represents the body moment of inertia tensor, M_{aero} defines the aerodynamic moments due to the wings, K_R and K_Ω are controller gains, and $M = [l, m, n]$ represents the desired control moment to be generated by the rotors. The derivation is omitted for brevity. The total thrust obtained from outer loop and the control moment from inner loop are converted into individual rotor thrust using mixer model (refer Fig. 5).

VI. Simulation Results

In this section, the performance of the proposed controller is demonstrated through 6-DOF dynamics simulation of forward and backward transitions. The NDI controller and geometric controller, acting as position control and attitude control respectively, are implemented on a 6-DOF vehicle dynamics system. The resulting control inputs, represented by individual rotor thrusts, are first validated to ensure they avoid saturation. The rotor thrusts are then transferred to the vehicle dynamics. The state of the UAV is described as conventional 12-D model with states ($X = [x, y, z, v_x, v_y, v_z, \phi, \theta, \psi, p, q, r]$). The fourth-order Runge-Kutta method integrates the system dynamics, iterating the states based on the control inputs and the current state. The performance of the controller under various conditions is evaluated by analyzing the deviation from the reference trajectory. The desired trajectory is shown by dashed lines and the achieved trajectory is shown in solid lines.

A. Performance under External Wind

The performance of the proposed NDI controller is evaluated under the influence of constant wind. Since the takeoff of any fixed-wing vehicle is typically performed against the wind, the external wind applied to the vehicle dynamics in simulation is directed opposite to the vehicle transition flight path. The performance is observed in both forward and backward transition.

1. Forward Transition

The vehicle is provided with the reference trajectory generated using optimization problem presented in Section IV.A. A steady wind with a magnitude of 1 m/s is applied to the vehicle dynamics along the *-ve* x-axis direction in inertial frame. The results are presented in Fig. 6. It can be seen that the UAV successfully tracks the position and velocity in inertial frame (refer Figs. 6a and 6b). There is slight rise in height, which is due to the presence of wind causing UAV to generate excess lift. By the end of the transition, the position error is converged to zero. To compensate for this error, the NDI controller modifies the pitch trajectory, as can be seen in Fig. 6c, the effect of which is observed in the pitchrate too. Rest of the states are not significantly affected due to disturbances.

2. Backward Transition

In the case of backwards transition, it is observed that the UAV is highly susceptible to external wind, as the vehicle is attempting to reach to a hover state. The UAV is able to handle wind speeds of upto only 0.5 m/s against the transition path. The results are presented in Fig. 7. It can be observed that the UAV smoothly transitions from cruise flight to hover. A slight disturbance is noted in tracking the velocity along the z-axis (refer Fig. 7b); however, once the UAV completes the backward transition, the risk of losing altitude is mitigated as the control thrust would be compensating the weights in hover condition.

On observing the forward and backward transition trajectories under external wind conditions, it can be concluded that the proposed NDI control can perform autonomous transition under wind conditions efficiently.

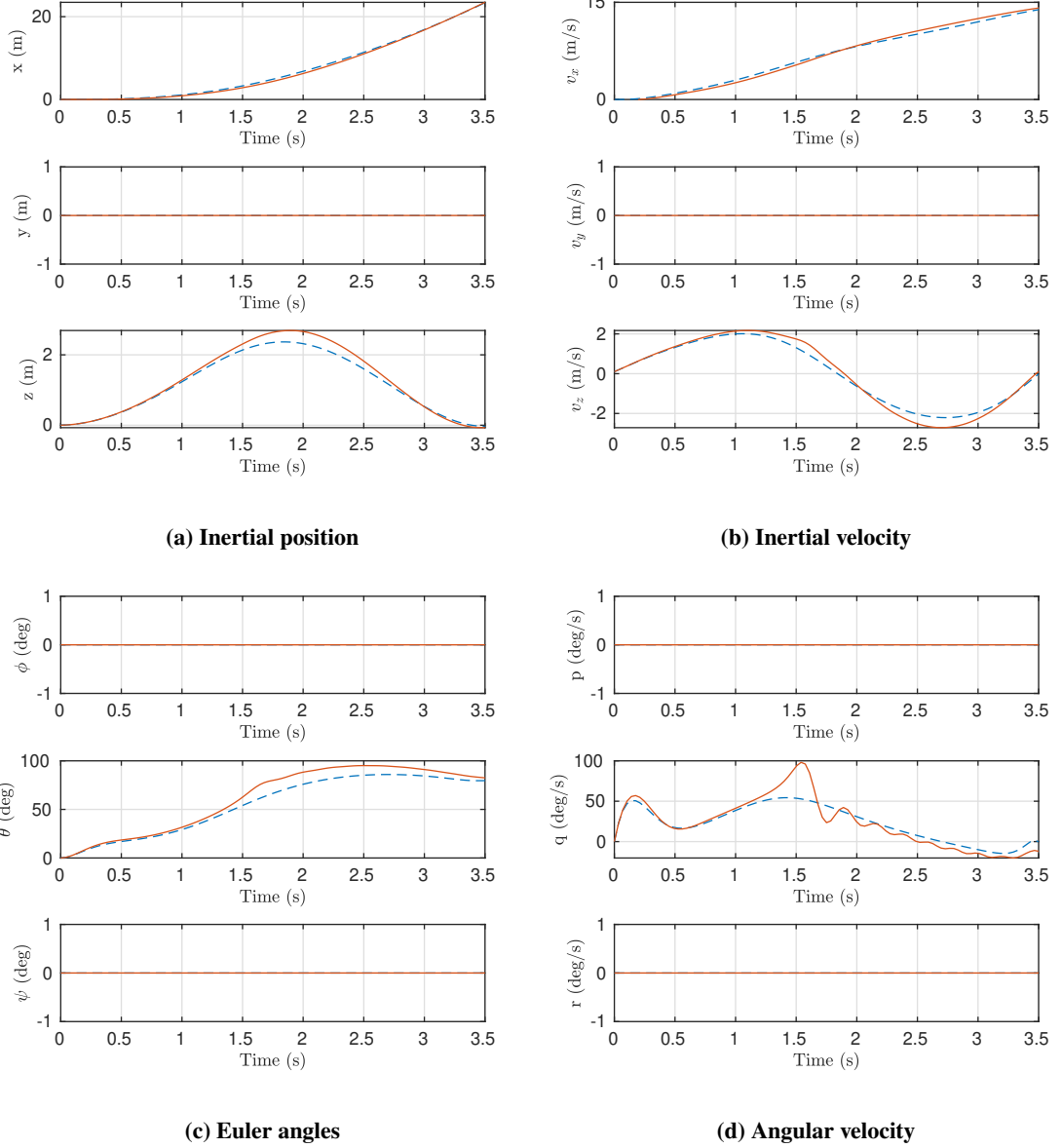
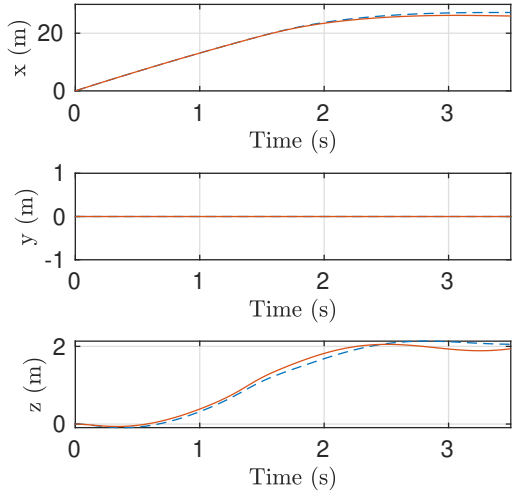
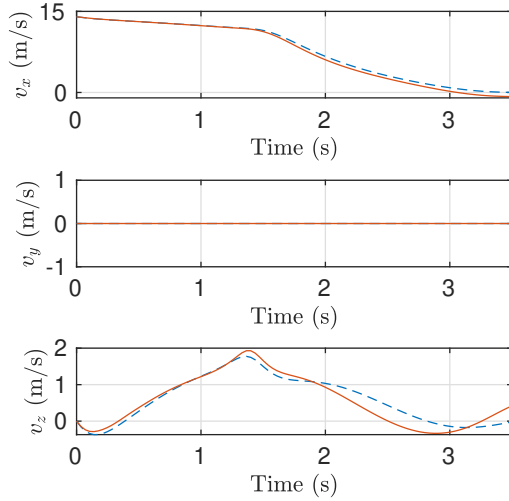


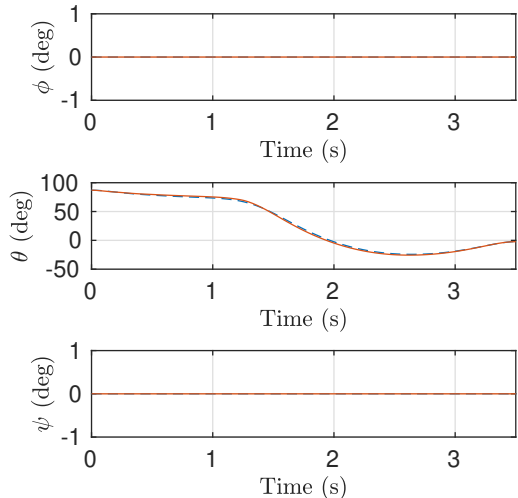
Fig. 6 NDI tracking control under steady wind during forward transition



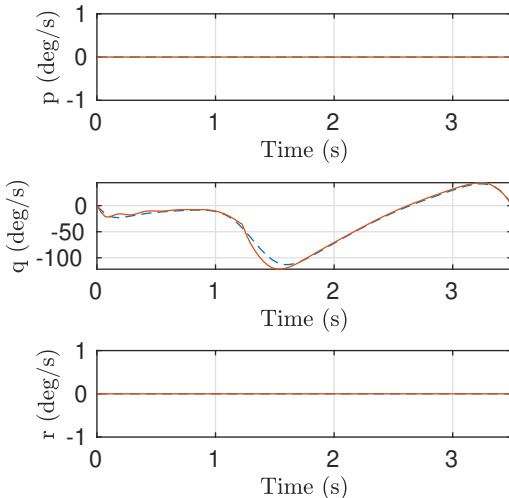
(a) Attitude and angular velocity



(b) Attitude and angular velocity



(c) Attitude and angular velocity



(d) Attitude and angular velocity

Fig. 7 NDI tracking control under steady wind during backward transition

B. Performance under System Uncertainties

The performance of the proposed NDI controller is evaluated under conditions of system uncertainties. To simulate the uncertainty in estimation of mathematical model of the system, we introduce random variations within a specific range to the physical parameters of the system. The deviation from the reference trajectory due to the difference between modeled and actual dynamics is fed to the NDI controller. The ability of the controller to successfully track the reference trajectory despite these uncertainties is assessed using Monte Carlo simulations. Figure 8 and Fig. 9 present the result of few such test cases for forward and backward transition, respectively. The specific parameter perturbations used in the simulation are given in Table 2.

Table 2 Parameter selection for forward and backward transition

Parameter	\bar{m}	J	C_{L_0}	C_{L_α}	C_{D_0}	C_{m_α}
Variation	$\pm 5\%$	$\pm 30\%$	$\pm 30\%$	$\pm 5\%$	$\pm 30\%$	$\pm 30\%$

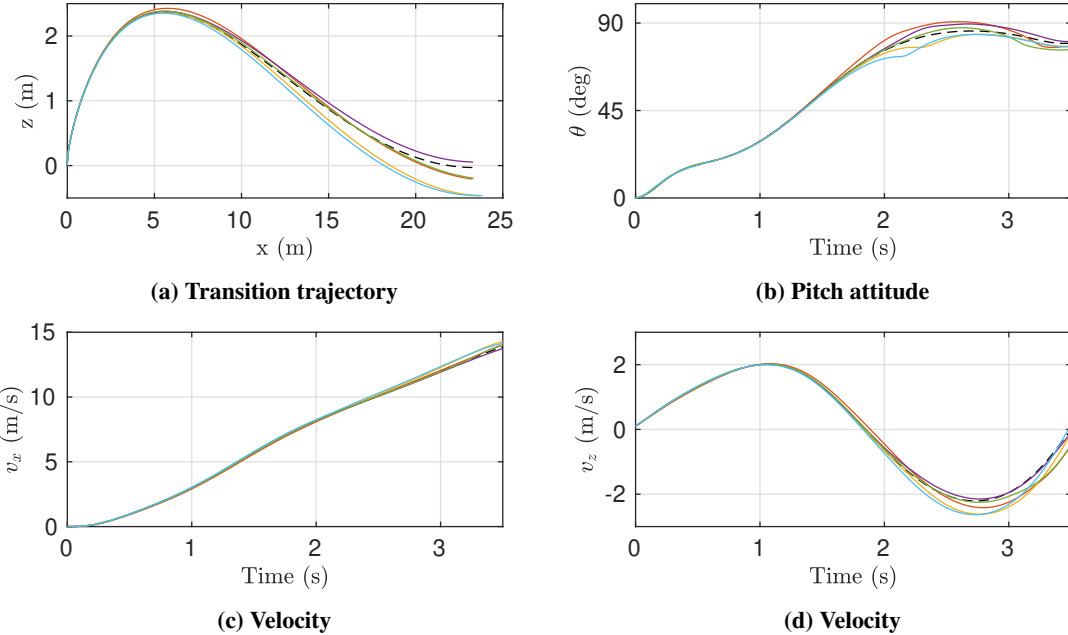


Fig. 8 Forward transition trajectory for five repeated tests

The Monte Carlo simulations revealed that the tracking performance of the proposed NDI controller is particularly sensitive to variations in mass \bar{m} and lift curve slope C_{L_α} . Consequently, we employed a smaller perturbation range (5%) for these two parameters compared to others. This difference can be justified as mass of a system can be determined with high accuracy, hence uncertainty in mass estimation barely arrives. Similarly, C_{L_α} is primarily influenced by the wing's airfoil structure, which is typically fixed during manufacturing and less prone to variations. Assembly misalignment may affect the zero angle-of-attack lift coefficient (C_{L_0}), but not the slope (C_{L_α}). Therefore, smaller perturbations for mass and lift curve slope reflects realistic scenarios with lower possibility of uncertainty.

As discussed earlier, a transition is considered successful when the vehicle achieves terminal velocity and attitude, without much loss/gain in altitude. The results of terminal states for 1000 simulations with parameter uncertainties are presented in Table 3 and Table 4. Mean is shown in bold letters, with standard deviation in brackets. It can be observed that the terminal state for transition is achieved efficiently with a slight variation under the presence of parameter uncertainties.

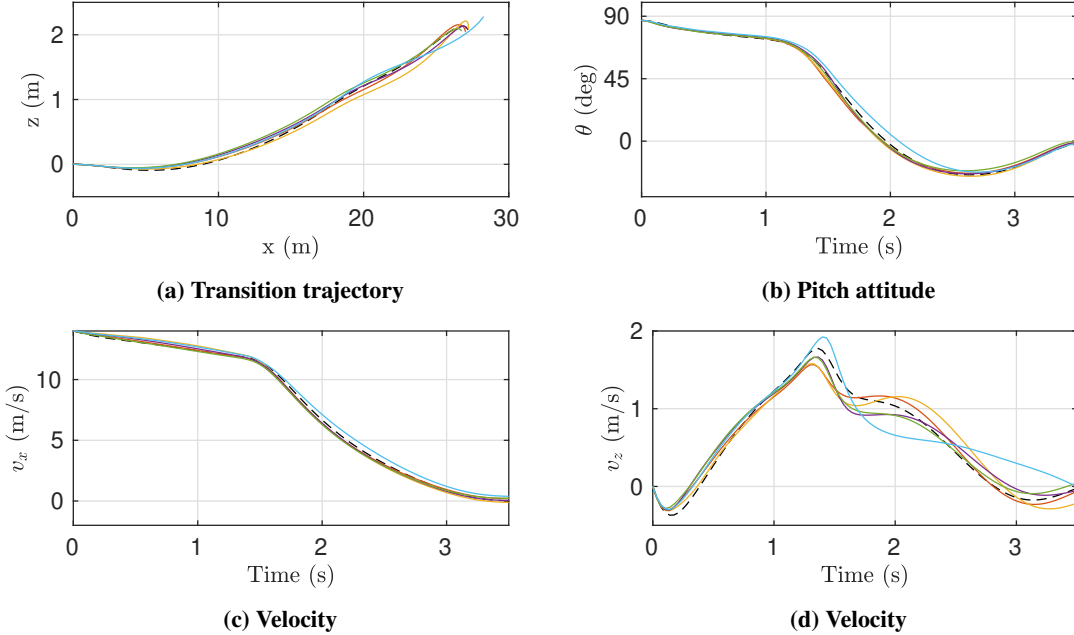


Fig. 9 Backward transition trajectory for five repeated tests

Table 3 Terminal states for forward transition

Parameter	Velocity (m/s)	Pitch (deg)	Altitude (m)
Desired Value	14	79.59	0
Simulation Result	14.26 (0.48)	79.16 (2.56)	-0.31 (0.34)

VII. Conclusion

The proposed work presents a closed loop nonlinear control strategy for optimal transition tracking of tailsitter UAVs. This approach involves generating reference transition trajectories for forward and backward flight using optimization methods. The proposed NDI controller is used to track the reference trajectories, while geometric control serves as inner loop attitude control. The performance of the proposed tracking controller was evaluated against non-zero wind conditions and system uncertainties in the model.

The evaluation yielded the following key findings regarding the controller's performance:

- The vehicle successfully performed forward transition under wind conditions of up to 1 m/s. However, backward transition proved more challenging in the presence of wind.
- Monte Carlo simulations performed to test the controller under uncertainties in various physical parameters revealed that the controller can track the reference trajectory efficiently even in the presence of parameter uncertainties in the model.
- Uncertainty in mass and lift curve slope are most difficult to deal with.

The simulation results demonstrate that the NDI controller enables the UAV to perform successful transitions while maintaining attitude and altitude stability. Furthermore, the controller exhibits robustness in handling uncertainties within the mathematical model. In future, the controller's performance could be evaluated with outdoor flight tests

Table 4 Terminal states for backward transition

Parameter	Velocity (m/s)	Pitch (deg)	Altitude (m)
Desired Value	0	0	2
Simulation Result	0.006 (0.12)	-2.38 (1.79)	2.10 (0.04)

incorporating wind gusts. This would provide valuable insights into the controller's robustness under challenging wind conditions.

References

- [1] Hassanalian, M., and Abdelkefi, A., "Classifications, applications, and design challenges of drones: A review," *Progress in Aerospace sciences*, Vol. 91, 2017, pp. 99–131.
- [2] Saeed, A. S., Younes, A. B., Cai, C., and Cai, G., "A survey of hybrid unmanned aerial vehicles," *Progress in Aerospace Sciences*, Vol. 98, 2018, pp. 91–105.
- [3] Ke, Y., Wang, K., and Chen, B. M., "Design and implementation of a hybrid UAV with model-based flight capabilities," *IEEE/ASME Transactions on Mechatronics*, Vol. 23, No. 3, 2018, pp. 1114–1125.
- [4] Abhishek, A., Krishna, M., Sinha, S., Bhowmik, J., and Das, D., "Design, development and flight testing of a novel quadrotor convertiplane unmanned air vehicle," *73rd Annual Forum of the American Helicopter Society*, AHS International, Inc. Fairfax, VA, 2017.
- [5] Chipade, V. S., Abhishek, Kothari, M., and Chaudhari, R. R., "Systematic design methodology for development and flight testing of a variable pitch quadrotor biplane VTOL UAV for payload delivery," *Mechatronics*, Vol. 55, 2018, pp. 94–114.
- [6] Raj, N., Banavar, R., Abhishek, and Kothari, M., "Attitude control of novel tail sitter: Swiveling biplane–quadrotor," *Journal of Guidance, Control, and Dynamics*, Vol. 43, No. 3, 2020, pp. 599–607.
- [7] Li, B., Sun, J., Zhou, W., Wen, C.-Y., Low, K. H., and Chen, C.-K., "Transition optimization for a VTOL tail-sitter UAV," *IEEE/ASME transactions on mechatronics*, Vol. 25, No. 5, 2020, pp. 2534–2545.
- [8] Gupta, S., Kothari, M., and Abhishek, "Optimal Transition Trajectory of a Quadrotor Biplane Tailsitter," *IFAC-PapersOnLine*, Vol. 56, No. 2, 2023, pp. 2500–2505. <https://doi.org/https://doi.org/10.1016/j.ifacol.2023.10.1230>, 22nd IFAC World Congress.
- [9] McIntosh, K., Reddinger, J.-P., Zhao, D., and Mishra, S., "Optimal trajectory generation for a quadrotor biplane tailsitter," *Vertical Flight Society 76th Annual Forum Proceedings*, 2020.
- [10] Verling, S., Stastny, T., Bättig, G., Alexis, K., and Siegwart, R., "Model-based transition optimization for a VTOL tailsitter," *2017 IEEE International Conference on Robotics and Automation (ICRA)*, IEEE, 2017, pp. 3939–3944.
- [11] Li, B., Sun, J., Zhou, W., Wen, C.-Y., Low, K. H., and Chen, C.-K., "Transition Optimization for a VTOL Tail-Sitter UAV," *IEEE/ASME Transactions on Mechatronics*, Vol. 25, No. 5, 2020, pp. 2534–2545. <https://doi.org/10.1109/TMECH.2020.2983255>.
- [12] Raj, N., Simha, A., Kothari, M., Abhishek, and Banavar, R. N., "Iterative Learning based feedforward control for Transition of a Biplane-Quadrotor Tailsitter UAS," *2020 IEEE International Conference on Robotics and Automation (ICRA)*, 2020, pp. 321–327. <https://doi.org/10.1109/ICRA40945.2020.9196671>.
- [13] Yang, Y., Yang, J., Wang, X., and Zhu, J., "Robust optimal transition maneuvers control for tail-sitter unmanned aerial vehicles," *International Journal of Robust and Nonlinear Control*, Vol. 31, No. 16, 2021, pp. 8007–8029.
- [14] Wang, K., Ke, Y., Lai, S., Gong, K., Tan, Y., and Chen, B. M., "Model-based optimal auto-transition and control synthesis for tail-sitter UAV KH-Lion," *2017 13th IEEE International Conference on Control & Automation (ICCA)*, IEEE, 2017, pp. 541–547.
- [15] Andersson, J. A. E., Gillis, J., Horn, G., Rawlings, J. B., and Diehl, M., "CasADi – A software framework for nonlinear optimization and optimal control," *Mathematical Programming Computation*, Vol. 11, No. 1, 2019, pp. 1–36. <https://doi.org/10.1007/s12532-018-0139-4>.
- [16] "Px4-tailsitter," , Jul. 2018. URL https://github.com/PX4/Firmware/blob/v1.8.0/src/modules/vtol_att_control/tailsitter.cpp, [Online].
- [17] Shastry, A. K., "A Universal Optimal Control Strategy for Biplane Quadrotor Tailsitter," Master's thesis, Indian Institute of Technology Kanpur, 2019.